ELSEVIER

Journal of Alloys and Compounds 434–435 (2007) 79–83

Journal of ALLOYS AND COMPOUNDS

www.elsevier.com/locate/jallcom

Mechanical behaviour of nanocomposites derived from zirconium based bulk amorphous alloys

S. Gravier [a], L. Charleux [a,b], A. Mussi [b,1], J.J. Blandin [a,*], P. Donnadieu [b], M. Verdier [b]

[a] *Génie Physique et Mécanique des Matériaux (GPM2), Institut National Polytechnique de Grenoble (INPG), ENSPG, UMR CNRS 5010, BP 46, 38402 Saint-Martin d'Hères Cedex, France*

[b] *Laboratoire Thermodynamique et Physico-Chimie Métallurgique (LTPCM), Institut National Polytechnique de Grenoble (INPG), ENSEEG, BP 75, 38402 Saint-Martin d'Hères Cedex, France*

Available online 9 October 2006

Abstract

The effects on mechanical properties of partial crystallization of a zirconium based bulk amorphous alloy (Vit1) are investigated. Nanocomposites are produced by appropriate heat treatments at temperatures higher than the glass transition temperature. Mechanical properties at room temperature are investigated by compression tests and hardness measurements including nanoindentation. The variation of the fracture stress with the degree of crystallinity is related to the nature, the size and the dispersion of the crystals in the amorphous phase. The variations of microstructure are estimated thanks to differential scanning calorimetry, X-ray diffraction and transmission electron microscopy. A significant connexion between crystals induces a decrease of the fracture stress whereas hardness continuously increases with crystallinity. From nanoindentation tests, Young's modulus and apparent yield stresses were roughly estimated and it is concluded that crystallization tends to increase the yield stress. Nevertheless, AFM observations of the imprints after indentation suggest that the mechanism of deformation can vary significantly with crystallization.

Keywords: Amorphous materials; Mechanical properties; Crystallization

1. Introduction

Bulk metallic glasses (BMG) exhibit interesting mechanical properties since they combine a high fracture stress, a particularly large elastic domain (up to 2%) and significant fracture toughness. An other interesting property of BMG is their ability to produce nanocomposite materials after heat treatments nearby the glass transition temperature T_g. Consequently, the effect of partial crystallization on the mechanical properties of BMG at room temperature has been also investigated [1,2]. Crystallization up to a critical level (often found nearby 30–40 vol. % of crystals [3]) generally results in an increase of the fracture stress σ_F and then to a drop of σ_F. This change is associated to a transition in fracture surface morphology from a well-developed vein pattern to cleavage like brittle facets. Conversely, hardness generally increases continuously with the degree of crystallization. This means that the σ_F drop is rather related to a loss of fracture resistance in the material than to a decrease of the yield stress. The aim of the present investigation is to study the impact of partial crystallization on the mechanical properties of the $Zr_{41.2}Ti_{13.8}Cu_{12.5}Ni_{10}Be_{22.5}$ (so-called Vit1) with a particular attention given to fracture stress and mechanisms of deformation.

2. Materials and experimental procedure

The Vit1 alloy was supplied by Howmet Corp. (USA) as 3.3 mm thick sheet. The differential scanning calorimetry (DSC) measurements were carried out in a Perkin-Elmer DSC at 10 K/min. The nature of the crystals was examined by X-ray diffraction (XRD, Cu Kα). Thin foils for TEM observations were prepared by ion beam milling (4 keV, 10°). The samples used for the compression tests where rods of 3 mm in diameter and tests were performed at an initial strain rate equal to $5 \times 10^{-4}\,s^{-1}$. The Vickers microhardness was measured with a 1000 g load. Nanoindentations were performed using a conical indenter with a maximum depth of 1.5 μm and loading and unloading deformation rates of $0.05\,s^{-1}$. The maximum acquisition rate was 5 Hz. Observations of the imprints were performed by atomic force microscopy (AFM).

* Corresponding author. Tel.: +33 476826341; fax: +33 476826382.
E-mail address: jean-jacques.blandin@inpg.fr (J.J. Blandin).

[1] Present address: LMP-SP2MI, BP 30179, 86962 Futuroscope Chasseneuil, France.

0925-8388/$ – see front matter © 2006 Elsevier B.V. All rights reserved.
doi:10.1016/j.jallcom.2006.08.113

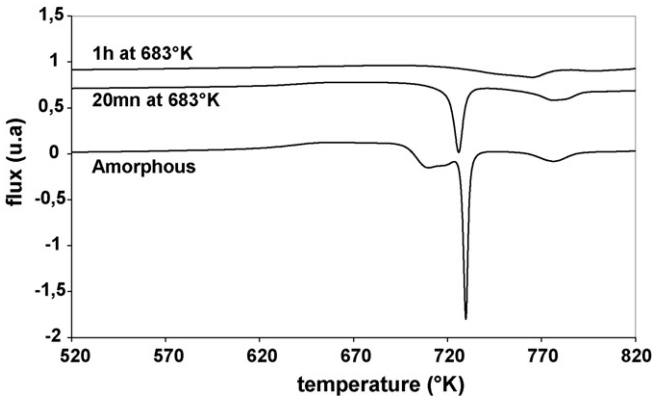

Fig. 1. DSC curves of Vit1 alloy after the selected heat treatments.

3. Investigated crystallized states

Fig. 1 shows the DSC curve of the amorphous alloy (state A) with the characteristic step change arising from glass transition (T_g corresponding to the inflexion point is equal to 637 K), followed by a super-cooled liquid region and then three exothermic peaks, respectively, at 705 K, 727 K and 774 K. These peaks are associated to three distinct crystallization events, keeping in mind that the first one can also include phase separation [4]. To study the effect of such crystallizations on the mechanical properties, three heat treatments have been selected and applied on the as-provided alloy: 20 min at 683 K (state B), 1 h at 683 K (state C) and 10 min at 823 K (state D). The DSC curve of the alloy in states B and C are also shown in Fig. 1: after 20 min annealing at 683 K, the first crystallization peak has disappeared while the crystallization peaks for the two other ones remain roughly unchanged. In the case of sample C, only the third peak is still present. One can note that despite some slight variations in characteristic temperatures of the peaks after heat treatments, their crystallization energies remains roughly unchanged.

4. Effect of crystallization on fracture stress

4.1. Compression tests

Fig. 2 shows the effect of the selected heat treatments on the fracture stresses σ_F measured during the compression tests at room temperature. Whatever the degree of crystallization, macroscopically brittle behaviours are obtained. The observed tendency confirms already published data about the effect of partial crystallization [3]: after a first increase, σ_F falls drastically. In parallel, the number of fragments in the broken sample increases rapidly from two pieces in samples A and B to nearly dusts in samples C and D. SEM observations of the broken samples confirm also the change in the fracture surface morphologies from the typical vein pattern for samples A and B to cleavage like facets for samples C and D.

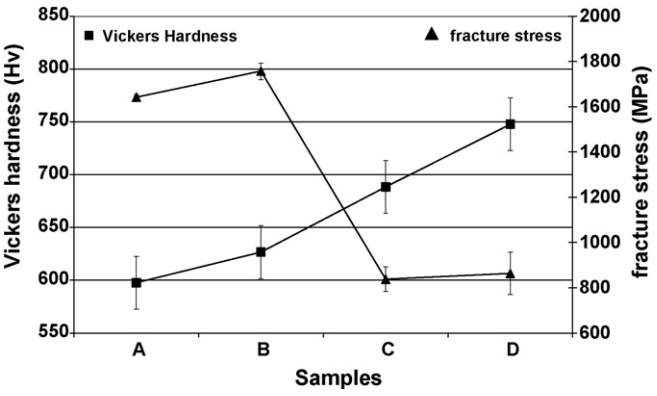

Fig. 2. Fracture stress σ_F and Vickers hardness for the four investigated samples.

4.2. Microstructural characterization

Fig. 3 displays dark field TEM observations of treated samples (B and D). In the case of sample B (Fig. 3(a)), dispersed crystals can be observed by TEM with an average size of 15 nm. Extending the maintain at 683 K (sample C) increases the number of crystals but without significant change of the average size.

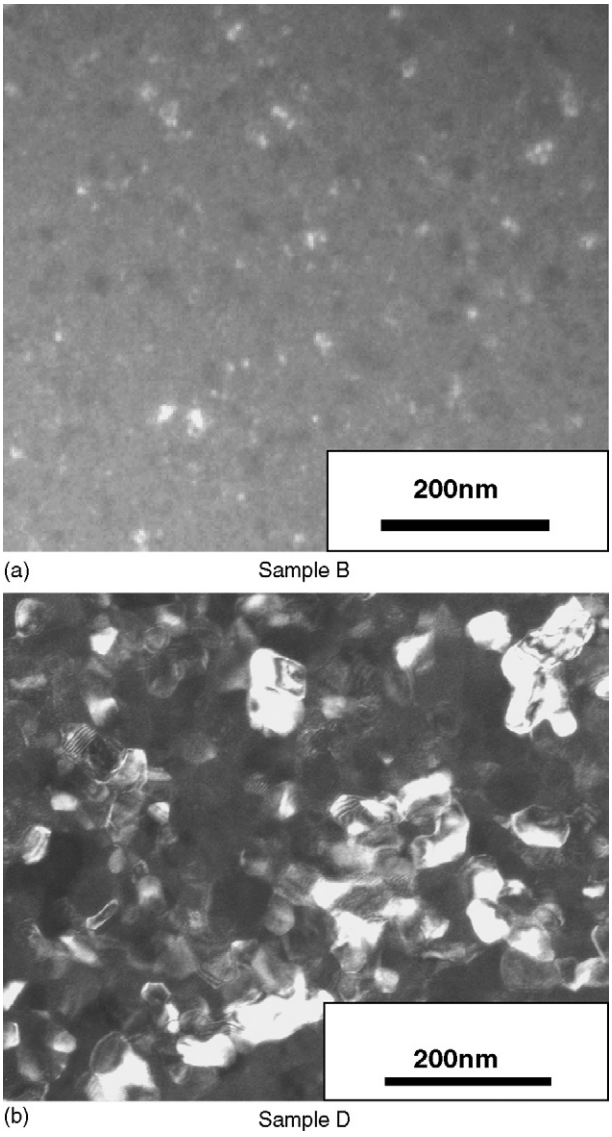

Fig. 3. TEM observations of samples B and D.

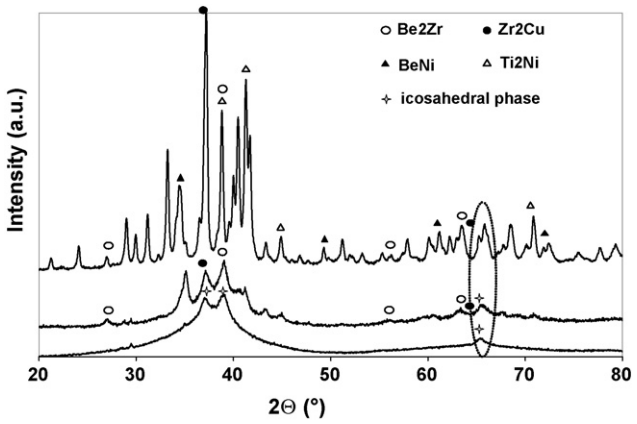

Fig. 4. X-ray patterns of Vit1 alloy after the selected heat treatments.

Grain boundaries were frequently detected in the TEM observations of sample D (Fig. 3(b)), meaning that the crystallization is nearly complete for this sample, with sizes typically close to 50 nm.

Fig. 4 shows the XRD profiles for the investigated conditions. The crystallization in sample B is confirmed since three main peaks can be identified and attributed to an icosahedral phase [4]. One can note that this icosahedral phase is still present after a longer maintain (sample C) as confirmed by TEM observation where typical five-fold symmetry of I-structure could still be observed or from the XRD spectrum since the third peak of the I phase does not disappear and has a similar height as for sample B. Additional peaks can also be detected in sample C, revealing the presence of Be_2Zr and Zr_2Cu [2,4,5]. Sample D exhibits many additional peaks, partly indexed by BeNi [4,6] and Ti_2Ni but all the crystalline phases have not been fully identified, confirming that the third peak is associated to a particularly complex crystallization process with probably overlapping peaks.

4.3. Relation between fracture stress and microstructure

As for other BMGs, the effect of crystallization on the fracture stress of the Vit1 alloy can be roughly divided in two main domains. When the population of crystals can be considered as a dispersion of particles in an amorphous matrix (as it is the case for sample B), the fracture surface morphology is similar to what is observed for the amorphous alloy and the fracture stress increases slightly with the degree of crystallization. In this case, the particles are expected to act as obstacles to the propagation of shear bands. In a second step, when connexions between particles are significant, an important drop in fracture stress is observed. This suggests that the Vit1 behaves in a quite similar way as other BMGs [3,7]. Specificities of the Vit1 are probably more related to the fact that crystallization in this alloy is particularly complex due to the large number of elements, the possibility to develop phase separation before primary crystallization, the presence of quasicrystals in a quite large crystallization domain (samples B and C) or the large variety of crystals coexisting for high degrees of crystallinity (sample D), which may favour intergranular fracture.

As already mentioned, the apparent stress–strain curves obtained during the compression tests displays the brittle like linear shape. In such macroscopic testing, the apparent fracture stress which is measured is not only related to local plasticity events but also to the fracture resistance. A way to get information about such local plasticity events is to carry out confined plastic deformation tests, like in hardness measurements.

5. Microhardness and nanoindentation tests

5.1. Microhardness

In Fig. 2 is also plotted the effect of crystallization on the Vickers microhardness. A maximum value close to 750 HV is obtained for the sample D, which is in agreement with values already reported for fully crystallized Vit1 (3 h at 873 K) [2]. The hardness tends to increase as crystallization proceeds with a maximum relative increase of about 25%. However, in microhardness tests, only the imprint after testing is available. More fruitful information can be obtained in nanoindentation tests since the variation of the load can be continuously measured as a function of the penetration depth.

5.2. Nanoindentation load versus penetration depth curves

The nanoindentation loading curves are shown in Fig. 5. For each condition, the reproducibility is excellent. One can note that the impact of crystallization on the nanoindentation curves for the four studied states remains limited. From such curves, two parameters can be deduced. Firstly, curves can usually be fitted by a parabolic law $P = Ch^2$ between the load P and the penetration depth h, with C a constant. The associated apparent hardness values are known to be proportional to the C constants. The relative variation of the apparent hardness with crystallization is given in Table 1. As for conventional microhardness measurements, a relative maximum increase of about 25% is still obtained. Secondly, the ratio of the plastic work W_{plast} over the total work W_{tot} can also be estimated. As far as crystallization occurs, the part of plastic deformation work in the total deformation work tends to decrease, from nearly 68% for sample A to about 63% for sample D.

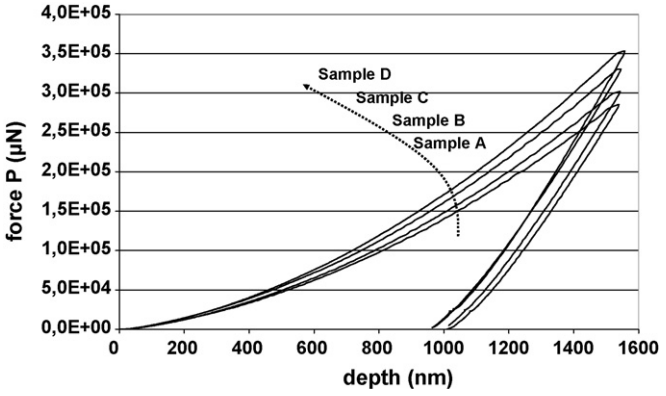

Fig. 5. Indentation load–displacement curves for the various annealed samples.

Table 1
Variation with microstructural state of the ratio W_{plast}/W_{tot}, the relative increase of apparent hardness and associated predictions of the Young's modulus and the yield stress (deduced from the numerical simulations under the assumption that $n = 0$)

	W_{plast}/W_{tot} (%)	$H/H_{amorphous}$	E (GPa)	σ_Y (GPa)
Amorphous (A)	67.9	1.00	105	2.6
20 min at 683 K (B)	66.1	1.07	109	2.9
1 h at 683 K (C)	64.1	1.18	115	3.4
10 min at 823 K (D)	63.1	1.23	118	3.6

5.3. Deduced Young's modulus and yield stress

The experimental data deduced from the nanoindentation loading–unloading curves derive from the elastic and plastic properties of the tested material. These properties can be rationalized thanks to three unknown parameters: the Young's modulus E, the yield stress σ_Y and the strain hardening (or softening) parameter n. In this framework, if a value of n is assumed, it would be possible to deduce E and σ_Y from the experimental data, using an appropriate finite element simulation. This procedure was carried out under the condition $n = 0$, which assumes no strain hardening or softening. In the case of the amorphous alloy, values of $E = 105$ GPa and $\sigma_Y = 2.6$ GPa are estimated. The value of E is in relatively good agreement with previously published data [8]. It is more delicate to comment the predicted value of σ_Y. This value is significantly higher than the fracture stress measured in compression but it is associated to confined plasticity and is consequently much less affected by the fracture mechanism. The assumption $n = 0$ was extended to the nanocrystallized structures and the resulting values of E and σ_Y are given in Table 1. The plastic behaviour of amorphous/nanocrystalline composites remains today poorly documented. Nevertheless, due to their nanometric size and their intermetallic nature, such crystals are expected to exhibit a very low hardening capacity. Consequently, as a first approximation, the assumption $n = 0$ was extended to the partially crystallized alloys. The relative increase in Young's modulus is very limited (less than 15%) whereas the apparent yield stress increases more significantly (from 2.6 GPa to 3.6 GPa). These results confirm the idea of an increased difficulty to initiate plasticity events when the degree of crystallinity increases. However, the values of σ_Y must be considered with caution. Indeed, quite large pressures (up to several GPa) are expected under the indenter and it is known that the mechanical properties of BMG are affected by pressure effects since it has been established that the Mohr–Coulomb criterion (with a pressure parameter α of about 0.1) was better adapted than the Von Mises one to account for the experimental mechanical properties of BMG [9]. However, in the present study, it must be kept in mind that these rough estimations were performed assuming $n = 0$ for all the studied structures, which assumes the same mechanism of deformation whatever the crystallization state. Fig. 6 shows AFM observations of the residual imprints in the case of samples A and D. The morphologies of these imprints are clearly different. In the case of sample A, one observes a pattern with an important residual pile up of about 100 nm and some discrete displacement jumps on the surface. This observation is in agreement with previously published AFM observations of imprints in the case of nanoindented amorphous alloys [10,11]. The sample D has a different pattern with a smaller residual pile up (of about 50 nm) and a smooth surface in the imprint. These observations suggest that the mechanisms of deformation are probably different between the investigated samples and that the value of the parameter n may probably vary with the degree of crystallization. Work is under progress to estimate such possible variations of n with the degree of crystallization.

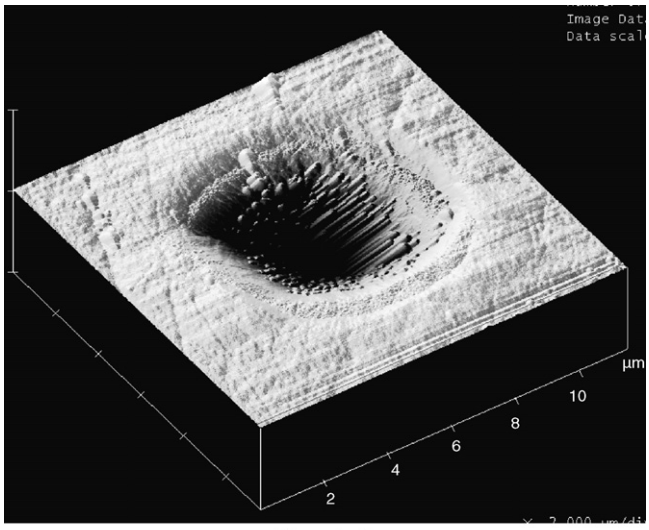

Sample A

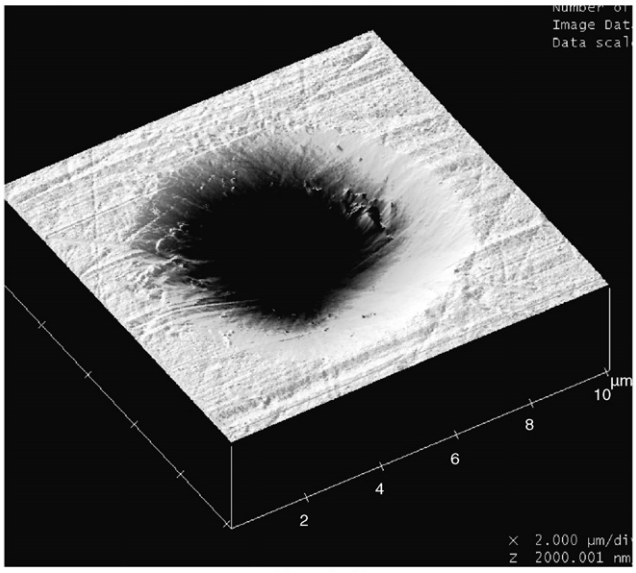

Sample D

Fig. 6. AFM observations of the nanoindentation imprints.

6. Conclusions

The effect of crystallization of Vit1 on the mechanical properties at room temperature was investigated thanks to uniaxial compression and nanoindentation tests. To get well-contrasted population of crystals, appropriate heat treatments have been

selected. When the degree of crystallization remains limited (typically less than 20% of ultra-fine quasi crystals), the fracture stress is slightly higher than for the amorphous alloy and the fracture surface morphology still exhibit a vein pattern. For large degrees of crystallization (for which a large variety of crystals is present with significant contacts between them), the fracture stress is sharply reduced and the fracture surface morphology is of cleavage type.

From nanoindentation tests, some information about the Young's modulus and an apparent yield stress can be obtained. Predictions, based on the assumption that all the studied samples exhibit the same strain hardening parameter support the idea that crystallization induces an important increase of the yield stress. However, AFM observations of the imprints suggest that the mechanism of deformation varies noticeably with crystallization.

References

[1] J. Eckert, A. Reger-Leonhard, B. Weiss, M. Heilmaier, L. Schultz, Adv. Eng. Mater. 3 (2001) 41.
[2] R.CY. Tam, C.H. Shek, Mater. Sci. Eng. A 364 (2004) 198.
[3] J. Basu, N. Nagendra, Y. Li, U. Ramamurty, Phil. Mag. 83 (2003) 1747.
[4] X.-P. Tang, J.F. Löffler, W.L. Johnson, Y. Wu, J. Non-Cryst. Solids 317 (2003) 118.
[5] I. Martin, T. Ohkubo, M. Ohnuma, B. Deconihout, K. Hono, Acta Mater. 52 (2004) 4427.
[6] Y.L. Gao, J. Shen, J.F. Sun, D.M. Chen, G. Wang, H.R. Wang, D.W. Xing, H.Z. Xian, B.D. Zhou, Mater. Lett. 57 (2003) 2341.
[7] Z. Bian, G. He, G.L. Chen, Scripta Mater. 43 (2000) 1003.
[8] J. Lu, G. Ravichandran, W.L. Johnson, Acta Mater. 51 (2003) 3429.
[9] R. Vaidyanathan, M. Dao, G. Ravichandran, S. Suresh, Acta Mater. 49 (2001) 3781.
[10] J.J. Kim, Y. Choi, S. Suresh, A.S. Argon, Science 295 (2002) 654.
[11] M.N.M. Patnaik, R. Narasimhan, U. Ramamurty, Acta Mater. 52 (2004) 3335–3345.